Search for Lepton Flavor Violation in the Decay $\tau^{\pm} \rightarrow e^{\pm}\gamma$

B. Aubert,[1] R. Barate,[1] D. Boutigny,[1] F. Couderc,[1] Y. Karyotakis,[1] J. P. Lees,[1] V. Poireau,[1] V. Tisserand,[1] A. Zghiche,[1] E. Grauges,[2] A. Palano,[3] M. Pappagallo,[3] A. Pompili,[3] J. C. Chen,[4] N. D. Qi,[4] G. Rong,[4] P. Wang,[4] Y. S. Zhu,[4] G. Eigen,[5] I. Ofte,[5] B. Stugu,[5] G. S. Abrams,[6] M. Battaglia,[6] A. B. Breon,[6] D. N. Brown,[6] J. Button-Shafer,[6] R. N. Cahn,[6] E. Charles,[6] C. T. Day,[6] M. S. Gill,[6] A. V. Gritsan,[6] Y. Groysman,[6] R. G. Jacobsen,[6] R. W. Kadel,[6] J. Kadyk,[6] L. T. Kerth,[6] Yu. G. Kolomensky,[6] G. Kukartsev,[6] G. Lynch,[6] L. M. Mir,[6] P. J. Oddone,[6] T. J. Orimoto,[6] M. Pripstein,[6] N. A. Roe,[6] M. T. Ronan,[6] W. A. Wenzel,[6] M. Barrett,[7] K. E. Ford,[7] T. J. Harrison,[7] A. J. Hart,[7] C. M. Hawkes,[7] S. E. Morgan,[7] A. T. Watson,[7] M. Fritsch,[8] K. Goetzen,[8] T. Held,[8] H. Koch,[8] B. Lewandowski,[8] M. Pelizaeus,[8] K. Peters,[8] T. Schroeder,[8] M. Steinke,[8] J. T. Boyd,[9] J. P. Burke,[9] N. Chevalier,[9] W. N. Cottingham,[9] T. Cuhadar-Donszelmann,[10] B. G. Fulsom,[10] C. Hearty,[10] N. S. Knecht,[10] T. S. Mattison,[10] J. A. McKenna,[10] A. Khan,[11] P. Kyberd,[11] M. Saleem,[11] L. Teodorescu,[11] A. E. Blinov,[12] V. E. Blinov,[12] A. D. Bukin,[12] V. P. Druzhinin,[12] V. B. Golubev,[12] E. A. Kravchenko,[12] A. P. Onuchin,[12] S. I. Serednyakov,[12] Yu. I. Skovpen,[12] E. P. Solodov,[12] A. N. Yushkov,[12] D. Best,[13] M. Bondioli,[13] M. Bruinsma,[13] M. Chao,[13] S. Curry,[13] I. Eschrich,[13] D. Kirkby,[13] A. J. Lankford,[13] P. Lund,[13] M. Mandelkern,[13] R. K. Mommsen,[13] W. Roethel,[13] D. P. Stoker,[13] C. Buchanan,[14] B. L. Hartfiel,[14] A. J. R. Weinstein,[14] S. D. Foulkes,[15] J. W. Gary,[15] O. Long,[15] B. C. Shen,[15] K. Wang,[15] L. Zhang,[15] D. del Re,[16] H. K. Hadavand,[16] E. J. Hill,[16] D. B. MacFarlane,[16] H. P. Paar,[16] S. Rahatlou,[16] V. Sharma,[16] J. W. Berryhill,[17] C. Campagnari,[17] A. Cunha,[17] B. Dahmes,[17] T. M. Hong,[17] M. A. Mazur,[17] J. D. Richman,[17] W. Verkerke,[17] T. W. Beck,[18] A. M. Eisner,[18] C. J. Flacco,[18] C. A. Heusch,[18] J. Kroseberg,[18] W. S. Lockman,[18] G. Nesom,[18] T. Schalk,[18] B. A. Schumm,[18] A. Seiden,[18] P. Spradlin,[18] D. C. Williams,[18] M. G. Wilson,[18] J. Albert,[19] E. Chen,[19] G. P. Dubois-Felsmann,[19] A. Dvoretskii,[19] D. G. Hitlin,[19] J. S. Minamora,[19] I. Narsky,[19] T. Piatenko,[19] F. C. Porter,[19] A. Ryd,[19] A. Samuel,[19] R. Andreassen,[20] G. Mancinelli,[20] B. T. Meadows,[20] M. D. Sokoloff,[20] F. Blanc,[21] P. Bloom,[21] S. Chen,[21] W. T. Ford,[21] J. F. Hirschauer,[21] A. Kreisel,[21] U. Nauenberg,[21] A. Olivas,[21] W. O. Ruddick,[21] J. G. Smith,[21] K. A. Ulmer,[21] S. R. Wagner,[21] J. Zhang,[21] A. Chen,[22] E. A. Eckhart,[22] A. Soffer,[22] W. H. Toki,[22] R. J. Wilson,[22] Q. Zeng,[22] D. Altenburg,[23] E. Feltresi,[23] A. Hauke,[23] B. Spaan,[23] T. Brandt,[24] J. Brose,[24] M. Dickopp,[24] V. Klose,[24] H. M. Lacker,[24] R. Nogowski,[24] S. Otto,[24] A. Petzold,[24] J. Schubert,[24] K. R. Schubert,[24] R. Schwierz,[24] J. E. Sundermann,[24] D. Bernard,[25] G. R. Bonneaud,[25] P. Grenier,[25] S. Schrenk,[25] Ch. Thiebaux,[25] G. Vasileiadis,[25] M. Verderi,[25] D. J. Bard,[26] P. J. Clark,[26] W. Gradl,[26] F. Muheim,[26] S. Playfer,[26] Y. Xie,[26] M. Andreotti,[27] V. Azzolini,[27] D. Bettoni,[27] C. Bozzi,[27] R. Calabrese,[27] G. Cibinetto,[27] E. Luppi,[27] M. Negrini,[27] L. Piemontese,[27] F. Anulli,[28] R. Baldini-Ferroli,[28] A. Calcaterra,[28] R. de Sangro,[28] G. Finocchiaro,[28] P. Patteri,[28] I. M. Peruzzi,[28,*] M. Piccolo,[28] A. Zallo,[28] A. Buzzo,[29] R. Capra,[29] R. Contri,[29] M. Lo Vetere,[29] M. Macri,[29] M. R. Monge,[29] S. Passaggio,[29] C. Patrignani,[29] E. Robutti,[29] A. Santroni,[29] S. Tosi,[29] G. Brandenburg,[30] K. S. Chaisanguanthum,[30] M. Morii,[30] E. Won,[30] J. Wu,[30] R. S. Dubitzky,[31] U. Langenegger,[31] J. Marks,[31] S. Schenk,[31] U. Uwer,[31] G. Schott,[32] W. Bhimji,[33] D. A. Bowerman,[33] P. D. Dauncey,[33] U. Egede,[33] R. L. Flack,[33] J. R. Gaillard,[33] J. A. Nash,[33] M. B. Nikolich,[33] W. Panduro Vazquez,[33] X. Chai,[34] M. J. Charles,[34] W. F. Mader,[34] U. Mallik,[34] A. K. Mohapatra,[34] V. Ziegler,[34] J. Cochran,[35] H. B. Crawley,[35] V. Eyges,[35] W. T. Meyer,[35] S. Prell,[35] E. I. Rosenberg,[35] A. E. Rubin,[35] J. Yi,[35] N. Arnaud,[36] M. Davier,[36] X. Giroux,[36] G. Grosdidier,[36] A. Höcker,[36] F. Le Diberder,[36] V. Lepeltier,[36] A. M. Lutz,[36] A. Oyanguren,[36] T. C. Petersen,[36] S. Plaszczynski,[36] S. Rodier,[36] P. Roudeau,[36] M. H. Schune,[36] A. Stocchi,[36] G. Wormser,[36] C. H. Cheng,[37] D. J. Lange,[37] M. C. Simani,[37] D. M. Wright,[37] A. J. Bevan,[38] C. A. Chavez,[38] I. J. Forster,[38] J. R. Fry,[38] E. Gabathuler,[38] R. Gamet,[38] K. A. George,[38] D. E. Hutchcroft,[38] R. J. Parry,[38] D. J. Payne,[38] K. C. Schofield,[38] C. Touramanis,[38] C. M. Cormack,[39] F. Di Lodovico,[39] W. Menges,[39] R. Sacco,[39] C. L. Brown,[40] G. Cowan,[40] H. U. Flaecher,[40] M. G. Green,[40] D. A. Hopkins,[40] P. S. Jackson,[40] T. R. McMahon,[40] S. Ricciardi,[40] F. Salvatore,[40] D. Brown,[41] C. L. Davis,[41] J. Allison,[42] N. R. Barlow,[42] R. J. Barlow,[42] C. L. Edgar,[42] M. C. Hodgkinson,[42] M. P. Kelly,[42] G. D. Lafferty,[42] M. T. Naisbit,[42] J. C. Williams,[42] C. Chen,[43] W. D. Hulsbergen,[43] A. Jawahery,[43] D. Kovalskyi,[43] C. K. Lae,[43] D. A. Roberts,[43] G. Simi,[43] G. Blaylock,[44] C. Dallapiccola,[44] S. S. Hertzbach,[44] R. Kofler,[44] V. B. Koptchev,[44] X. Li,[44] T. B. Moore,[44] S. Saremi,[44] H. Staengle,[44] S. Willocq,[44] R. Cowan,[45] K. Koeneke,[45] G. Sciolla,[45] S. J. Sekula,[45] M. Spitznagel,[45] F. Taylor,[45] R. K. Yamamoto,[45] H. Kim,[46] P. M. Patel,[46] S. H. Robertson,[46] A. Lazzaro,[47] V. Lombardo,[47] F. Palombo,[47] J. M. Bauer,[48] L. Cremaldi,[48] V. Eschenburg,[48] R. Godang,[48] R. Kroeger,[48] J. Reidy,[48] D. A. Sanders,[48] D. J. Summers,[48] H. W. Zhao,[48] S. Brunet,[49] D. Côté,[49] P. Taras,[49] B. Viaud,[49] H. Nicholson,[50] N. Cavallo,[51,†] G. De Nardo,[51] F. Fabozzi,[51,‡] C. Gatto,[51] L. Lista,[51] D. Monorchio,[51] P. Paolucci,[51] D. Piccolo,[51] C. Sciacca,[51] M. Baak,[52] H. Bulten,[52] G. Raven,[52] H. L. Snoek,[52] L. Wilden,[52] C. P. Jessop,[53] J. M. LoSecco,[53] T. Allmendinger,[54] G. Benelli,[54]

0031-9007/06/96(4)/041801(7)$23.00

K. K. Gan,[54] K. Honscheid,[54] D. Hufnagel,[54] P. D. Jackson,[54] H. Kagan,[54] R. Kass,[54] T. Pulliam,[54] A. M. Rahimi,[54] R. Ter-Antonyan,[54] Q. K. Wong,[54] J. Brau,[55] R. Frey,[55] O. Igonkina,[55] M. Lu,[55] C. T. Potter,[55] N. B. Sinev,[55] D. Strom,[55] J. Strube,[55] E. Torrence,[55] F. Galeazzi,[56] M. Margoni,[56] M. Morandin,[56] M. Posocco,[56] M. Rotondo,[56] F. Simonetto,[56] R. Stroili,[56] C. Voci,[56] M. Benayoun,[57] H. Briand,[57] J. Chauveau,[57] P. David,[57] L. Del Buono,[57] Ch. de la Vaissière,[57] O. Hamon,[57] M. J. J. John,[57] Ph. Leruste,[57] J. Malclès,[57] J. Ocariz,[57] L. Roos,[57] G. Therin,[57] P. K. Behera,[58] L. Gladney,[58] Q. H. Guo,[58] J. Panetta,[58] M. Biasini,[59] R. Covarelli,[59] S. Pacetti,[59] M. Pioppi,[59] C. Angelini,[60] G. Batignani,[60] S. Bettarini,[60] F. Bucci,[60] G. Calderini,[60] M. Carpinelli,[60] R. Cenci,[60] F. Forti,[60] M. A. Giorgi,[60] A. Lusiani,[60] G. Marchiori,[60] M. Morganti,[60] N. Neri,[60] E. Paoloni,[60] M. Rama,[60] G. Rizzo,[60] J. Walsh,[60] M. Haire,[61] D. Judd,[61] D. E. Wagoner,[61] J. Biesiada,[62] N. Danielson,[62] P. Elmer,[62] Y. P. Lau,[62] C. Lu,[62] J. Olsen,[62] A. J. S. Smith,[62] A. V. Telnov,[62] F. Bellini,[63] G. Cavoto,[63] A. D'Orazio,[63] E. Di Marco,[63] R. Faccini,[63] F. Ferrarotto,[63] F. Ferroni,[63] M. Gaspero,[63] L. Li Gioi,[63] M. A. Mazzoni,[63] S. Morganti,[63] G. Piredda,[63] F. Polci,[63] F. Safai Tehrani,[63] C. Voena,[63] H. Schröder,[64] G. Wagner,[64] R. Waldi,[64] T. Adye,[65] N. De Groot,[65] B. Franek,[65] G. P. Gopal,[65] E. O. Olaiya,[65] F. F. Wilson,[65] R. Aleksan,[66] S. Emery,[66] A. Gaidot,[66] S. F. Ganzhur,[66] G. Graziani,[66] G. Hamel de Monchenault,[66] W. Kozanecki,[66] M. Legendre,[66] G. W. London,[66] B. Mayer,[66] G. Vasseur,[66] Ch. Yèche,[66] M. Zito,[66] M. V. Purohit,[67] A. W. Weidemann,[67] J. R. Wilson,[67] F. X. Yumiceva,[67] T. Abe,[68] M. T. Allen,[68] D. Aston,[68] R. Bartoldus,[68] N. Berger,[68] A. M. Boyarski,[68] O. L. Buchmueller,[68] R. Claus,[68] J. P. Coleman,[68] M. R. Convery,[68] M. Cristinziani,[68] J. C. Dingfelder,[68] D. Dong,[68] J. Dorfan,[68] D. Dujmic,[68] W. Dunwoodie,[68] S. Fan,[68] R. C. Field,[68] T. Glanzman,[68] S. J. Gowdy,[68] T. Hadig,[68] V. Halyo,[68] C. Hast,[68] T. Hryn'ova,[68] W. R. Innes,[68] M. H. Kelsey,[68] P. Kim,[68] M. L. Kocian,[68] D. W. G. S. Leith,[68] J. Libby,[68] S. Luitz,[68] V. Luth,[68] H. L. Lynch,[68] H. Marsiske,[68] R. Messner,[68] D. R. Muller,[68] C. P. O'Grady,[68] V. E. Ozcan,[68] A. Perazzo,[68] M. Perl,[68] B. N. Ratcliff,[68] A. Roodman,[68] A. A. Salnikov,[68] R. H. Schindler,[68] J. Schwiening,[68] A. Snyder,[68] J. Stelzer,[68] D. Su,[68] M. K. Sullivan,[68] K. Suzuki,[68] S. K. Swain,[68] J. M. Thompson,[68] J. Va'vra,[68] N. van Bakel,[68] M. Weaver,[68] W. J. Wisniewski,[68] M. Wittgen,[68] D. H. Wright,[68] A. K. Yarritu,[68] K. Yi,[68] C. C. Young,[68] P. R. Burchat,[69] A. J. Edwards,[69] S. A. Majewski,[69] B. A. Petersen,[69] C. Roat,[69] M. Ahmed,[70] S. Ahmed,[70] M. S. Alam,[70] R. Bula,[70] J. A. Ernst,[70] M. A. Saeed,[70] F. R. Wappler,[70] S. B. Zain,[70] W. Bugg,[71] M. Krishnamurthy,[71] S. M. Spanier,[71] R. Eckmann,[72] J. L. Ritchie,[72] A. Satpathy,[72] R. F. Schwitters,[72] J. M. Izen,[73] I. Kitayama,[73] X. C. Lou,[73] S. Ye,[73] F. Bianchi,[74] M. Bona,[74] F. Gallo,[74] D. Gamba,[74] M. Bomben,[75] L. Bosisio,[75] C. Cartaro,[75] F. Cossutti,[75] G. Della Ricca,[75] S. Dittongo,[75] S. Grancagnolo,[75] L. Lanceri,[75] L. Vitale,[75] F. Martinez-Vidal,[76] R. S. Panvini,[77] Sw. Banerjee,[78] B. Bhuyan,[78] C. M. Brown,[78] D. Fortin,[78] K. Hamano,[78] R. Kowalewski,[78] J. M. Roney,[78] R. J. Sobie,[78] J. J. Back,[79] P. F. Harrison,[79] T. E. Latham,[79] G. B. Mohanty,[79] H. R. Band,[80] X. Chen,[80] B. Cheng,[80] S. Dasu,[80] M. Datta,[80] A. M. Eichenbaum,[80] K. T. Flood,[80] M. Graham,[80] J. J. Hollar,[80] J. R. Johnson,[80] P. E. Kutter,[80] H. Li,[80] R. Liu,[80] B. Mellado,[80] A. Mihalyi,[80] Y. Pan,[80] M. Pierini,[80] R. Prepost,[80] P. Tan,[80] S. L. Wu,[80] Z. Yu,[80] and H. Neal[81]

(*BaBar* Collaboration)

[1]*Laboratoire de Physique des Particules, F-74941 Annecy-le-Vieux, France*
[2]*IFAE, Universitat Autonoma de Barcelona, E-08193 Bellaterra, Barcelona, Spain*
[3]*Dipartimento di Fisica and INFN, Università di Bari, I-70126 Bari, Italy*
[4]*Institute of High Energy Physics, Beijing 100039, China*
[5]*Institute of Physics, University of Bergen, N-5007 Bergen, Norway*
[6]*Lawrence Berkeley National Laboratory and University of California, Berkeley, California 94720, USA*
[7]*University of Birmingham, Birmingham, B15 2TT, United Kingdom*
[8]*Institut für Experimentalphysik 1, Ruhr Universität Bochum, D-44780 Bochum, Germany*
[9]*University of Bristol, Bristol BS8 1TL, United Kingdom*
[10]*University of British Columbia, Vancouver, British Columbia, Canada V6T 1Z1*
[11]*Brunel University, Uxbridge, Middlesex UB8 3PH, United Kingdom*
[12]*Budker Institute of Nuclear Physics, Novosibirsk 630090, Russia*
[13]*University of California at Irvine, Irvine, California 92697, USA*
[14]*University of California at Los Angeles, Los Angeles, California 90024, USA*
[15]*University of California at Riverside, Riverside, California 92521, USA*
[16]*University of California at San Diego, La Jolla, California 92093, USA*
[17]*University of California at Santa Barbara, Santa Barbara, California 93106, USA*
[18]*Institute for Particle Physics, University of California at Santa Cruz, Santa Cruz, California 95064, USA*
[19]*California Institute of Technology, Pasadena, California 91125, USA*
[20]*University of Cincinnati, Cincinnati, Ohio 45221, USA*

[21]University of Colorado, Boulder, Colorado 80309, USA
[22]Colorado State University, Fort Collins, Colorado 80523, USA
[23]Institut für Physik, Universität Dortmund, D-44221 Dortmund, Germany
[24]Institut für Kern- und Teilchenphysik, Technische Universität Dresden, D-01062 Dresden, Germany
[25]Ecole Polytechnique, LLR, F-91128 Palaiseau, France
[26]University of Edinburgh, Edinburgh EH9 3JZ, United Kingdom
[27]Dipartimento di Fisica and INFN, Università di Ferrara, I-44100 Ferrara, Italy
[28]Laboratori Nazionali di Frascati dell'INFN, I-00044 Frascati, Italy
[29]Dipartimento di Fisica and INFN, Università di Genova, I-16146 Genova, Italy
[30]Harvard University, Cambridge, Massachusetts 02138, USA
[31]Physikalisches Institut, Universität Heidelberg, Philosophenweg 12, D-69120 Heidelberg, Germany
[32]Institut für Experimentelle Kernphysik, Universität Karlsruhe, D-76021 Karlsruhe, Germany
[33]Imperial College London, London, SW7 2AZ, United Kingdom
[34]University of Iowa, Iowa City, Iowa 52242, USA
[35]Iowa State University, Ames, Iowa 50011-3160, USA
[36]Laboratoire de l'Accélérateur Linéaire, F-91898 Orsay, France
[37]Lawrence Livermore National Laboratory, Livermore, California 94550, USA
[38]University of Liverpool, Liverpool L69 72E, United Kingdom
[39]Queen Mary, University of London, London E1 4NS, United Kingdom
[40]Royal Holloway and Bedford New College, University of London, Egham, Surrey TW20 0EX, United Kingdom
[41]University of Louisville, Louisville, Kentucky 40292, USA
[42]University of Manchester, Manchester M13 9PL, United Kingdom
[43]University of Maryland, College Park, Maryland 20742, USA
[44]University of Massachusetts, Amherst, Massachusetts 01003, USA
[45]Laboratory for Nuclear Science, Massachusetts Institute of Technology, Cambridge, Massachusetts 02139, USA
[46]McGill University, Montréal, Québec, Canada H3A 2T8
[47]Dipartimento di Fisica and INFN, Università di Milano, I-20133 Milano, Italy
[48]University of Mississippi, University, Mississippi 38677, USA
[49]Laboratoire René J. A. Lévesque, Université de Montréal, Montréal, Québec, Canada H3C 3J7
[50]Mount Holyoke College, South Hadley, Massachusetts 01075, USA
[51]Dipartimento di Scienze Fisiche and INFN, Università di Napoli Federico II, I-80126, Napoli, Italy
[52]NIKHEF, National Institute for Nuclear Physics and High Energy Physics, NL-1009 DB Amsterdam, The Netherlands
[53]University of Notre Dame, Notre Dame, Indiana 46556, USA
[54]The Ohio State University, Columbus, Ohio 43210, USA
[55]University of Oregon, Eugene, Oregon 97403, USA
[56]Dipartimento di Fisica and INFN, Università di Padova, I-35131 Padova, Italy
[57]Laboratoire de Physique Nucléaire et de Hautes Energies, Universités Paris VI et VII, F-75252 Paris, France
[58]University of Pennsylvania, Philadelphia, Pennsylvania 19104, USA
[59]Dipartimento di Fisica and INFN, Università di Perugia, I-06100 Perugia, Italy
[60]Dipartimento di Fisica, Scuola Normale Superiore and INFN, Università di Pisa, I-56127 Pisa, Italy
[61]Prairie View A&M University, Prairie View, Texas 77446, USA
[62]Princeton University, Princeton, New Jersey 08544, USA
[63]Dipartimento di Fisica and INFN,Università di Roma La Sapienza, I-00185 Roma, Italy
[64]Universität Rostock, D-18051 Rostock, Germany
[65]Rutherford Appleton Laboratory, Chilton, Didcot, Oxon OX11 0QX, United Kingdom
[66]DSM/Dapnia, CEA/Saclay, F-91191 Gif-sur-Yvette, France
[67]University of South Carolina, Columbia, South Carolina 29208, USA
[68]Stanford Linear Accelerator Center, Stanford, California 94309, USA
[69]Stanford University, Stanford, California 94305-4060, USA
[70]State University of New York, Albany, New York 12222, USA
[71]University of Tennessee, Knoxville, Tennessee 37996, USA
[72]University of Texas at Austin, Austin, Texas 78712, USA
[73]University of Texas at Dallas, Richardson, Texas 75083, USA
[74]Dipartimento di Fisica Sperimentale and INFN, Università di Torino, I-10125 Torino, Italy
[75]Dipartimento di Fisica and INFN, Università di Trieste, I-34127 Trieste, Italy
[76]IFIC, Universitat de Valencia-CSIC, E-46071 Valencia, Spain
[77]Vanderbilt University, Nashville, Tennessee 37235, USA
[78]University of Victoria, Victoria, British Columbia, Canada V8W 3P6
[79]Department of Physics, University of Warwick, Coventry CV4 7AL, United Kingdom
[80]University of Wisconsin, Madison, Wisconsin 53706, USA
[81]Yale University, New Haven, Connecticut 06511, USA

(Received 5 August 2005; published 2 February 2006)

A search for the nonconservation of lepton flavor in the decay $\tau^{\pm} \rightarrow e^{\pm}\gamma$ has been performed with 2.07×10^8 $e^+e^- \rightarrow \tau^+\tau^-$ events collected by the *BABAR* detector at the SLAC PEP II storage ring at a center-of-mass energy near 10.58 GeV. We find no evidence for a signal and set an upper limit on the branching ratio of $\mathcal{B}(\tau^{\pm} \rightarrow e^{\pm}\gamma) < 1.1 \times 10^{-7}$ at 90% confidence level.

DOI: 10.1103/PhysRevLett.96.041801 PACS numbers: 13.35.Dx, 11.30.Hv, 14.60.Fg

Lepton flavor conservation differs from other conservation laws in the standard model (SM) because it is not associated with an underlying conserved current symmetry. Consequently, new theories attempting to describe nature beyond the SM often include lepton flavor violating processes such as the neutrinoless decay of a μ or τ lepton, which have long been identified as unambiguous signatures of new physics. If no specific theoretical model is assumed, any or all of the $\mu \rightarrow e\gamma$, $\tau \rightarrow \mu\gamma$, and $\tau \rightarrow e\gamma$ decays can be expected to be observed, and therefore independent searches for each of these modes are required. Some theoretical models [1,2] respecting the current limits on $\mathcal{B}(\mu^+ \rightarrow e^+\gamma)$ [3] and $\mathcal{B}(\tau^{\pm} \rightarrow \mu^{\pm}\gamma)$ [4], in fact, allow $\tau^{\pm} \rightarrow e^{\pm}\gamma$ decays to occur up to the existing experimental bound [5].

A significant improvement on this $\tau^{\pm} \rightarrow e^{\pm}\gamma$ limit is presented here using data recorded by the *BABAR* detector at the SLAC PEP II asymmetric-energy e^+e^- storage ring. The data sample consists of an integrated luminosity of $\mathcal{L} = 210.6\ \mathrm{fb}^{-1}$ recorded at a center-of-mass (c.m.) energy ($\sqrt{s}$) of $\sqrt{s} = 10.58$ GeV, and $21.6\ \mathrm{fb}^{-1}$ recorded at $\sqrt{s} = 10.54$ GeV. With an average cross section of $\sigma_{e^+e^- \rightarrow \tau^+\tau^-} = (0.89 \pm 0.02)$ nb [6] as determined using the KK2F Monte Carlo (MC) generator [7], this corresponds to a data sample of 2.07×10^8 τ-pair events.

The *BABAR* detector is described in detail in Ref. [8]. Charged particles are reconstructed as tracks with a 5-layer silicon vertex tracker and a 40-layer drift chamber (DCH) inside a 1.5 T solenoidal magnet. An electromagnetic calorimeter (EMC) consisting of 6580 CsI(Tl) crystals is used to identify electrons and photons. A ring-imaging Cherenkov detector (DIRC) is used to identify charged hadrons and provides additional electron identification information.

The signature of the signal process is the presence of an isolated $e\gamma$ pair having an invariant mass consistent with that of the τ (1.777 GeV$/c^2$ [9]) and a total energy ($E_{e\gamma}$) equal to $\sqrt{s}/2$ in the c.m. frame, along with other particles in the event with properties consistent with a SM τ decay. Such events are simulated with higher-order radiative corrections using the KK2F MC generator [7] where one τ decays into $e\gamma$ according to phase space [10], while the other τ decays according to measured branching ratios [11] simulated with the TAUOLA MC generator [12,13]. The detector response is simulated with the GEANT4 package [14]. The simulated events for signal as well as SM background processes [7,12,13,15–17] are then reconstructed in the same manner as data. The MC backgrounds are used to optimize the selection criteria and study systematic errors in the efficiency estimates, but not for the estimation of the final background rate, which relies solely on data. For the background from Bhabha events, we do not rely upon MC predictions because the large Bhabha cross section makes generation of a sufficiently large MC sample impractical.

Events with zero total charge and with two or four well-reconstructed tracks inconsistent with coming from a photon conversion are selected. The event is divided into hemispheres by the plane perpendicular to the thrust axis. The thrust axis, which characterizes the direction of maximum energy flow in the c.m. frame of the event [18], is calculated using all observed charged and neutral particles.

The signal-side hemisphere is required to contain at least one γ with a c.m. energy greater than 500 MeV, and one track identified as an electron. The electron identification uses DCH, EMC, and DIRC information, including a requirement that the E/p ratio (the energy deposited in the EMC by the charged particle divided by its momentum as measured in the DCH) lies between 0.89 and 1.2. The electron candidate is required to lie within the fiducial acceptance of the EMC and to have a momentum greater than 500 MeV$/c$. These criteria yield a π misidentification rate of less than 0.3%. The efficiency for correctly identifying reconstructed tracks in the fiducial volume as electrons in $\tau^{\pm} \rightarrow e^{\pm}\gamma$ MC events is greater than 91%. For events with more than one signal-side γ candidate, we choose the γ that gives the mass of the $e\gamma$ system closest to the τ mass. This provides the correct pairing for 99.9% of selected signal MC events.

The resolution of the $e\gamma$ mass is improved by assigning the point of closest approach of the e track to the e^+e^- collision axis as the origin of the γ candidate and by using a kinematic fit with $E_{e\gamma}$ constrained to $\sqrt{s}/2$. The resulting energy-constrained mass (m_{EC}) and $\Delta E = E_{e\gamma} - \sqrt{s}/2$ are independent variables apart from small correlations arising from initial and final state radiation. The mean and standard deviation of the m_{EC} and ΔE distributions for reconstructed MC signal events are $\langle m_{\mathrm{EC}} \rangle = 1777\ \mathrm{MeV}/c^2$, $\sigma(m_{\mathrm{EC}}) = 9\ \mathrm{MeV}/c^2$, $\langle \Delta E \rangle = -15$ MeV, and $\sigma(\Delta E) = 51$ MeV where the shift in $\langle \Delta E \rangle$ comes from photon energy reconstruction effects. To minimize possible biases, we perform a blind analysis by excluding all events in the data within a $\pm 3\sigma$ rectangular box centered on $\langle m_{\mathrm{EC}} \rangle$ and $\langle \Delta E \rangle$ until all optimization and systematic studies of the selection criteria have been completed. We optimize the selection to obtain the smallest expected upper limit in a background-only hypothesis for observing events inside a $\pm 2\sigma$ rectangular box signal box defined by $|\Delta E - \langle \Delta E \rangle| < 2\sigma(\Delta E)$ and $|m_{EC} - m_\tau| < 2\sigma(m_{EC})$, as shown in Fig. 1.

The dominant backgrounds arise from Bhabha and $e^+e^- \to \tau^+\tau^-$ (with a $\tau \to e\nu\bar{\nu}$ decay) processes with an energetic γ from initial or final state radiation or from $\tau \to e\nu\bar{\nu}\gamma$ decays. Backgrounds arising from radiation are reduced by requiring that the total c.m. energy of all non-signal γ candidates in the signal-side hemisphere be less than 200 MeV. To suppress non-τ backgrounds with significant radiation along the beam directions, the polar angle ($\theta_{\rm miss}$) of the missing momentum associated with the neutrino(s) in the event is required to lie within the detector acceptance ($-0.76 < \cos\theta_{\rm miss} < 0.92$).

The tag-side hemisphere, defined to be that opposite to the signal-side hemisphere, is expected to contain a SM τ decay characterized by the presence of one or three charged particles and missing momentum due to unobserved neutrino(s). Taking the direction of the tag-side τ to be opposite the signal $e\gamma$ candidate, we use all tracks and γ candidates in the tag-side hemisphere to calculate the invariant mass squared of the tag-side missing momentum (m_ν^2), which peaks around zero for the signal. To reduce backgrounds from radiative $e^+e^- \to \tau^+\tau^-$ processes, we require $m_\nu^2 > -0.25\ \mathrm{GeV}^2/c^4$.

The component of the missing momentum of the event transverse to the collision axis scaled to the beam energy ($2 \times p^T_{\rm miss}/\sqrt{s}$) is expected to be large for signal and $e^+e^- \to \tau^+\tau^-$ events, but small for Bhabha and 2-photon events. We exploit an observed correlation between m_ν^2 and ($2 \times p^T_{\rm miss}/\sqrt{s}$) in the non-$\tau$ backgrounds to significantly suppress them. We require the following: $(m_\nu^2/1.8\ \mathrm{GeV}^2/c^4) - \ln(2 \times p^T_{\rm miss}/\sqrt{s})/2.0 < 1$, the highest c.m. momentum track on the tag-side hemisphere to be inconsistent with being an electron, including requirements that E/p be less than 0.5 and that the momentum be greater than 500 MeV/c, and the tag-side hemisphere to have a total c.m. momentum of all charged and neutral particles less than 4.75 GeV/c.

Backgrounds from $e^+e^- \to q\bar{q}$ processes are further reduced by requiring the total invariant mass of particles in the tag-side hemisphere to be less than 1.8 GeV/c^2.

After this selection, 8.9% of the total generated MC signal events survive within a grand signal box (GSB) region defined as follows: $m_{EC} \in [1.5, 2.0]$ GeV/c^2, $\Delta E \in [-1.0, 0.5]$ GeV. The data distribution of m_{EC} and ΔE inside the GSB is plotted as dots in Fig. 1, along with a shaded region containing 50% of the selected signal MC events shown for illustrative purposes. The GSB excluding the $\pm 3\sigma$ blind region contains 1110 data events, while the luminosity-normalized sum of the non-Bhabha MC backgrounds yield 1045 events. Of these MC events, 99.8% are $e^+e^- \to \tau^+\tau^-$ events, 99.9% of which have $\tau \to e\nu\bar{\nu}$ decays on the signal side.

The $(5.9 \pm 3.7)\%$ difference between the number of data and τ-pair dominated MC events indicates that the Bhabha background level in the GSB is low. However, in the more restrictive $|\Delta E - \langle \Delta E \rangle| < 2\sigma(\Delta E)$ region, the Bhabha background is expected to contribute a substantially higher background fraction because of the greater likelihood of a Bhabha than a τ-pair event to have a hemisphere containing the full beam energy. This residual Bhabha contamination is studied using data distributions of the deviation (ΔE_γ) of the measured photon c.m. energy from the corresponding prediction assuming a fully contained $e^+e^- \to e^+e^-\gamma$ event. The predicted photon energy is obtained from the beam energy and kinematic information from all particles in the event except the measured photon energy. We observe that the excess of data over non-Bhabha MC events is clustered at low ΔE_γ, where the Bhabha events are expected to appear. As we progressively loosen the electron veto on the tag-side track, the excess in the number of data events over the non-Bhabha MC background grows in the region with small ΔE_γ, providing further confirmation that the Bhabha background is well understood.

We cross-check the Bhabha contamination in the $|\Delta E - \langle \Delta E \rangle| < 2\sigma(\Delta E)$ region from a data sample without a tag-side electron veto, by removing the E/p requirement on the tag side. To estimate the Bhabha contamination surviving our final event selection, which includes a cut of tag side $E/p < 0.5$, we use the data in the adjacent Bhabha-dominated E/p region, $0.5 < E/p < 1.2$. We extrapolate the rate from the $0.5 < E/p < 1.2$

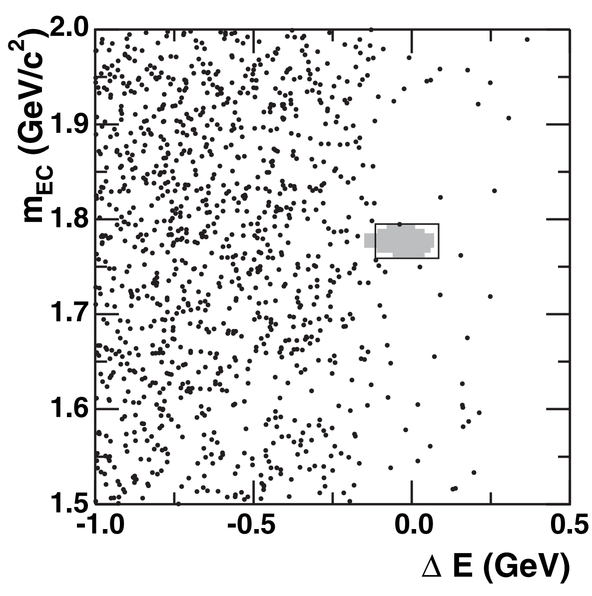

FIG. 1. m_{EC} vs ΔE distribution of data (dots) and shaded region containing 50% of the selected signal MC events inside the grand signal box, as defined in the text. The boundary of the $\pm 2\sigma$ signal box is also shown.

region to the $E/p < 0.5$ region, using a high statistics and high purity Bhabha control sample obtained by reversing the requirement on $(m_\nu^2/1.8\ \mathrm{GeV}^2/c^4) - \ln(2 \times p_{\mathrm{miss}}^T/\sqrt{s})/2.0$ given above. We estimate the residual Bhabha contamination in our final selection by multiplying the number of events in the $0.5 < E/p < 1.2$ region of the no tag-side electron veto sample by the ratio of the number of events in the Bhabha control sample in the $E/p < 0.5$ region to that in the $0.5 < E/p < 1.2$ region. This method gives an estimate of 10.3 ± 1.1 Bhabha events inside the $\pm 2\sigma(\Delta E)$ band once the tag-side electron veto is applied.

In this band, we expect 12.9 ± 2.5 events from the non-Bhabha MC backgrounds, thus obtaining a total background estimate of 23.2 ± 2.7 events. This compares well with the 25 events observed inside the $\pm 2\sigma(\Delta E)$ band in the data. We also find good agreement between the observed and expected number of events separately for the subsamples with one and three tracks on the tag side.

For the final background estimate we use the m_{EC} distribution of data events inside the $\pm 2\sigma(\Delta E)$ band, as shown in Fig. 2 along with the signal shape included for illustrative purposes. The backgrounds from data inside the $\pm 2\sigma(\Delta E)$ band with $|m_{\mathrm{EC}} - m_\tau| > 3\sigma(m_{\mathrm{EC}})$ are fitted to different orders of polynomials in m_{EC} using a maximum likelihood approach. A fit with a constant probability density function (PDF) yields a total χ^2 of 4.7 for the 10 bins shown in Fig. 2, and predicts 1.9 ± 0.4 events inside the final $\pm 2\sigma(m_{\mathrm{EC}})$ signal region. Equally acceptable goodness of fit is obtained with higher-order polynomials. However, the coefficients of the higher-order terms are statistically compatible with zero. The background predictions from these PDFs agree with the prediction from the constant PDF to within ± 0.3 events. As these deviations are smaller than the statistical error on the prediction from the constant PDF, we conclude that the data m_{EC} distribution is consistent with being uniform.

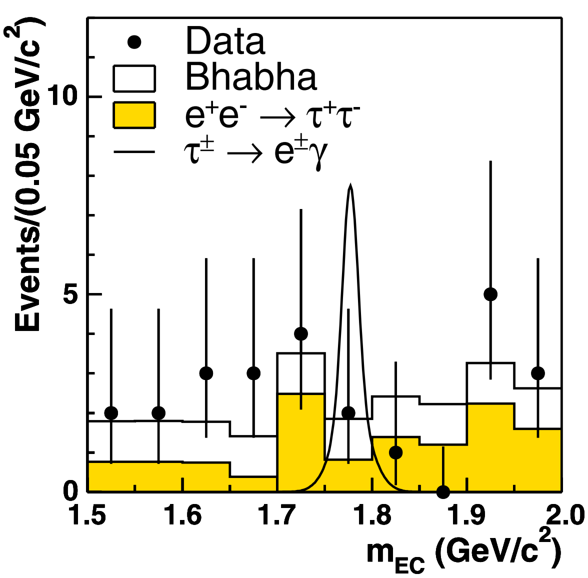

FIG. 2 (color online). m_{EC} distribution of data (dots), the expected backgrounds (histograms), and MC signal (curve with arbitrary normalization) for $|\Delta E - \langle \Delta E \rangle| < 2\sigma(\Delta E)$.

A cross-check using non-Bhabha MC background contributions combined with residual Bhabha contamination estimates obtained from the data is also found to be reasonably uniform in m_{EC} (Fig. 2) and predicts 1.7 ± 0.2 events inside the $\pm 2\sigma(m_{\mathrm{EC}})$ signal box.

The $(5.9 \pm 3.7)\%$ difference between data and τ-pair MC predictions also provides a measure of our ability to model the signal-like events in the GSB, since these data events have very similar characteristics to the signal, both in terms of the trigger response of the experiment as well as for the distributions of all the selection variables apart from m_{EC} and ΔE. The systematic error due to a particular cut is taken as the product of the marginal efficiency of the cut and the relative discrepancy between data and MC in the GSB after all other cuts have been applied. The contributions from all the different cuts added in quadrature yield a 2.3% relative systematic error, the only appreciable effect being associated with the requirements on m_ν^2 and p_{miss}^T. This approach yields a more conservative estimate of the systematic uncertainty on the signal efficiency than the more traditional approach derived from considering the difference between the data and MC prediction for each selection variable, which gives a total estimate of 2.0% relative contribution from all the cuts.

The relative systematic uncertainties on the trigger efficiency, tracking and photon reconstruction efficiencies, and particle identification are estimated to be 1.4%, 1.3%, 1.8%, and 1.3%, respectively. The requirement that the events fall within the $\pm 2\sigma$ signal box in m_{EC} and ΔE contributes a 4.4% systematic error associated with the scale and resolution uncertainties of these variables and a small contribution from the beam energy uncertainty. As we use 1.3×10^6 MC signal events, the contribution to the uncertainty arising from signal MC statistics is negligible. Adding the contributions of the individual terms in quadrature with an additional 2.3% normalization error on the product $\mathcal{L}\sigma_{\tau\tau}$ gives a 6.2% total relative systematic uncertainty on $\mathcal{L}\sigma_{\tau\tau}\varepsilon$ in the signal box, where the efficiency is $\varepsilon = (4.7 \pm 0.3)\%$. We note that our final limit on the branching ratio is insensitive to the systematic uncertainty as long as this uncertainty is below 10%.

We find one event in the signal box for an expected background of 1.9 ± 0.4 events. Because of the low background levels, we do not fit for a signal in the m_{EC} distribution as is done in our recent search for $\tau^\pm \to \mu^\pm\gamma$ [4]. Rather, we set an upper limit employing the same technique used in our search for $\tau^\pm \to \ell^\pm\ell^+\ell^-$ [19] where the background levels were also small. A 90% C.L. upper limit on the branching ratio is calculated according to $\mathcal{B}_{\mathrm{UL}}^{90} = N_{\mathrm{UL}}^{90}/(2\varepsilon\mathcal{L}\sigma_{\tau\tau})$, where N_{UL}^{90} is the 90% C.L. upper limit

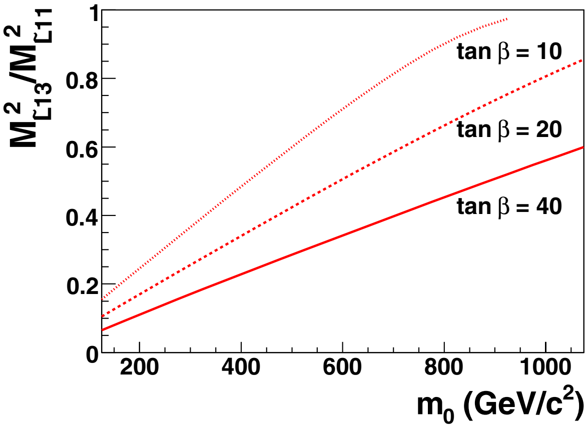

FIG. 3 (color online). Upper limits of 90% C.L. on $M^2_{\tilde{L}13}/M^2_{\tilde{L}11}$ for $\mathcal{B}(\tau^\pm \to e^\pm \gamma) < 1.1 \times 10^{-7}$ with $\tan\beta = 10$, 20, and 40.

with one event observed when 1.9 ± 0.4 events are expected. The limit is calculated including all uncertainties using the technique of Cousins and Highland [20] following the implementation of Barlow [21]. At 90% C.L. this procedure gives an upper limit of $\mathcal{B}(\tau^\pm \to e^\pm \gamma) < 1.1 \times 10^{-7}$ [22]. This represents a more than threefold reduction in the upper limit as reported in [5].

As an example of how this result constrains theories beyond the SM, we set bounds on the ratio of the first and the third generation elements to the first generation diagonal element ($M^2_{\tilde{L}13}/M^2_{\tilde{L}11}$) of the left-handed slepton mass matrix based on predictions from a minimal supergravity model [23,24]. Figure 3 shows the upper limits on $M^2_{\tilde{L}13}/M^2_{\tilde{L}11}$ as a function of the ratio of the Higgs vacuum expectation values ($\tan\beta$) and the universal scalar mass (m_0), which, for simplicity, is set equal to the universal gaugino mass.

We are grateful for the excellent luminosity and machine conditions provided by our PEP II colleagues, and for the substantial dedicated effort from the computing organizations that support *BABAR*. The collaborating institutions thank SLAC for its support and kind hospitality. This work is supported by DOE and NSF (USA), NSERC (Canada), IHEP (China), CEA and CNRS-IN2P3 (France), BMBF and DFG (Germany), INFN (Italy), FOM (The Netherlands), NFR (Norway), MIST (Russia), and PPARC (United Kingdom). Individuals have received support from the A. P. Sloan Foundation, Research Corporation, and Alexander von Humboldt Foundation.

*Also with Università di Perugia, Dipartimento di Fisica, Perugia, Italy.
†Also with Università della Basilicata, Potenza, Italy.
‡Deceased.

[1] E. Ma, Nucl. Phys. B, Proc. Suppl. **123**, 125 (2003).
[2] J. R. Ellis, J. Hisano, M. Raidal, and Y. Shimizu, Phys. Rev. D **66**, 115013 (2002).
[3] M. L. Brooks *et al.* (MEGA Collaboration), Phys. Rev. Lett. **83**, 1521 (1999). $\mathcal{B}(\mu^+ \to e^+ \gamma) < 1.2 \times 10^{-11}$ at 90% C.L.
[4] B. Aubert *et al.* (*BABAR* Collaboration), Phys. Rev. Lett. **95**, 041802 (2005). $\mathcal{B}(\tau^\pm \to \mu^\pm \gamma) < 6.8 \times 10^{-8}$ at 90% C.L.
[5] K. Hayasaka *et al.* (Belle Collaboration), Phys. Lett. B **613**, 20 (2005). $\mathcal{B}(\tau^\pm \to e^\pm \gamma) < 3.9 \times 10^{-7}$ at 90% C.L.
[6] The uncertainty was conservatively estimated by comparing cross sections from KK2F [7] and KORALB: S. Jadach and Z. Was, Comput. Phys. Commun. **85**, 453 (1995).
[7] B. F. Ward, S. Jadach, and Z. Was, Nucl. Phys. B, Proc. Suppl. **116**, 73 (2003).
[8] B. Aubert *et al.* (*BABAR* Collaboration), Nucl. Instrum. Methods Phys. Res., Sect. A **479**, 1 (2002).
[9] J. Z. Bai *et al.* (BES Collaboration), Phys. Rev. D **53**, 20 (1996).
[10] Our limit is insensitive to the phase space assumption as cross-checked with the two extreme cases of a $V - A$ and a $V + A$ form of interaction for the signal MC.
[11] S. Eidelman *et al.* (Particle Data Group), Phys. Lett. B **592**, 1 (2004).
[12] S. Jadach, Z. Was, R. Decker, and J. H. Kuhn, Comput. Phys. Commun. **76**, 361 (1993).
[13] E. Barberio and Z. Was, Comput. Phys. Commun. **79**, 291 (1994).
[14] S. Agostinelli *et al.* (GEANT4 Collaboration), Nucl. Instrum. Methods Phys. Res., Sect. A **506**, 250 (2003).
[15] D. J. Lange, Nucl. Instrum. Methods Phys. Res., Sect. A **462**, 152 (2001).
[16] T. Sjöstrand, Comput. Phys. Commun. **82**, 74 (1994).
[17] S. Jadach, W. Placzek, and B. F. L. Ward, Phys. Lett. B **390**, 298 (1997).
[18] S. Brandt *et al.*, Phys. Lett. **12**, 57 (1964); E. Fahri, Phys. Rev. Lett. **39**, 1587 (1977).
[19] B. Aubert *et al.* (*BABAR* Collaboration), Phys. Rev. Lett. **92**, 121801 (2004).
[20] R. D. Cousins and V. L. Highland, Nucl. Instrum. Methods Phys. Res., Sect. A **320**, 331 (1992).
[21] R. Barlow, Comput. Phys. Commun. **149**, 97 (2002).
[22] For an equivalent toy MC experiment with no signal, the expected upper limit at 90% C.L. is $\mathcal{B}(\tau^\pm \to e^\pm \gamma) < 1.2 \times 10^{-7}$, similar to that obtained in Ref. [4].
[23] A. Brignole and A. Rossi, Nucl. Phys. **B701**, 3 (2004).
[24] W. Porod, Comput. Phys. Commun. **153**, 275 (2003).